JCI The Journal of Clinical Investigation

PINCH1 regulates Akt1 activation and enhances radioresistance by inhibiting PP1α

Iris Eke, … , Reinhard Fässler, Nils Cordes

J Clin Invest. 2010;120(7):2516-2527. https://doi.org/10.1172/JCI41078.

Research Article Oncology

Tumor cell resistance to ionizing radiation and chemotherapy is a major obstacle in cancer therapy. One factor contributing to this is integrin-mediated adhesion to ECM. The adapter protein particularly interesting new cysteine-histidine-rich 1 (PINCH1) is recruited to integrin adhesion sites and promotes cell survival, but the mechanisms underlying this effect are not well understood. Here we have shown that PINCH1 is expressed at elevated levels in human tumors of diverse origins relative to normal tissue. Furthermore, PINCH1 promoted cell survival upon treatment with ionizing radiation in vitro and in vivo by perpetuating Akt1 phosphorylation and activity. Mechanistically, PINCH1 was found to directly bind to protein phosphatase 1α (PP1α) — an Akt1-regulating protein — and inhibit PP1α activity, resulting in increased Akt1 phosphorylation and enhanced radioresistance. Thus, our data suggest that targeting signaling molecules such as PINCH1 that function downstream of focal adhesions (the complexes that mediate tumor cell adhesion to ECM) may overcome radio- and chemoresistance, providing new therapeutic approaches for cancer.

PINCH1 regulates Akt1 activation and enhances radioresistance by inhibiting PP1α

Iris Eke,[1] Ulrike Koch,[1] Stephanie Hehlgans,[1] Veit Sandfort,[1] Fabio Stanchi,[2] Daniel Zips,[1,3] Michael Baumann,[1,3] Anna Shevchenko,[4] Christian Pilarsky,[5] Michael Haase,[6,7] Gustavo B. Baretton,[7] Véronique Calleja,[8] Banafshé Larijani,[8] Reinhard Fässler,[2] and Nils Cordes[1]

[1]OncoRay — Center for Radiation Research in Oncology, Medical Faculty Carl Gustav Carus, Dresden University of Technology, Dresden, Germany. [2]Department of Molecular Medicine, Max Planck Institute of Biochemistry, Martinsried, Germany. [3]Department of Radiation Oncology, University Hospital and Medical Faculty Carl Gustav Carus, Dresden University of Technology, Dresden, Germany. [4]Max Planck Institute of Molecular Cell Biology and Genetics, Dresden, Germany. [5]Department of Visceral, Thoracic, and Vascular Surgery, [6]Department of Pediatric Surgery, and [7]Institute of Pathology, University Hospital and Medical Faculty Carl Gustav Carus, Dresden University of Technology, Dresden, Germany. [8]Cell Biophysics Laboratory, Lincoln's Inn Fields Laboratories, London Research Institute, Cancer Research UK, London, United Kingdom.

Tumor cell resistance to ionizing radiation and chemotherapy is a major obstacle in cancer therapy. One factor contributing to this is integrin-mediated adhesion to ECM. The adapter protein particularly interesting new cysteine-histidine-rich 1 (PINCH1) is recruited to integrin adhesion sites and promotes cell survival, but the mechanisms underlying this effect are not well understood. Here we have shown that PINCH1 is expressed at elevated levels in human tumors of diverse origins relative to normal tissue. Furthermore, PINCH1 promoted cell survival upon treatment with ionizing radiation in vitro and in vivo by perpetuating Akt1 phosphorylation and activity. Mechanistically, PINCH1 was found to directly bind to protein phosphatase 1α (PP1α) — an Akt1-regulating protein — and inhibit PP1α activity, resulting in increased Akt1 phosphorylation and enhanced radioresistance. Thus, our data suggest that targeting signaling molecules such as PINCH1 that function downstream of focal adhesions (the complexes that mediate tumor cell adhesion to ECM) may overcome radio- and chemoresistance, providing new therapeutic approaches for cancer.

Introduction

Mutations in proto-oncogenes or tumor suppressors like Ras and p53, alteration in apoptosis signaling, and changes in the tumor microenvironment are common traits of tumor cell resistance to therapy (1–6), resulting in cancer stem cell survival and tumor recurrence (7). In combination with surgery and chemotherapy, more than 50% of cancer patients receive radiotherapy with high curative potential resulting from permanent local tumor control. In recent years, radiotherapy achieved additional success in local tumor control and cancer cure by the identification and targeting of molecules that critically regulate the radiation response of tumor cells (7–9). As molecules of focal adhesions (FAs), which mediate cell-ECM interactions, essentially contribute to radio- and chemoresistance of tumor cells (1, 10, 11), the present study aimed to identify further potent therapeutic cancer targets associated with FAs.

The major components of FAs are integrins, growth factor receptors, cytoplasmic signaling, and adapter molecules, which coalesce to a large membrane-associated multiprotein structure and signaling hub to control critical cell functions including survival, proliferation, migration, and cancer therapy response (1, 9, 12, 13). Among the essential regulators of FA function are the 5 Lin-1, Isl-1, Mec-3 (LIM) domain–containing particularly interesting new cysteine-histidine-rich 1 (PINCH1) and PINCH2 proteins (14). In avian and mouse models, PINCH1 has been shown to be critical for cell survival, spreading, adhesion, and migration by forming a ternary protein complex with integrin-linked kinase (ILK) and parvin (13, 15). Furthermore, the PINCH proteins have also been shown to bind Nck adapter protein 2 (Nck2; ref. 16), Ras suppressor protein 1 (Rsu1; ref. 17), and thymosin β4 (18). In concert with transmembrane integrin and growth factor receptors, the PINCH/ILK/parvin complex enables cooperative signaling for the regulation of cell survival via the PI3K/PKB/Akt1 and Ras/MAPK cascades (17, 19).

Akt1 plays a central role in apoptosis, tumor progression, resistance to cancer therapy, and radiation survival response (20–22). PI3K-dependent Akt1 activation by integrins and growth factor receptors through phosphorylation at amino acid residues S473 and T308 precedes Akt1-dependent phosphorylation of downstream targets such as forkhead box O (FoxO) transcription factors, glycogen synthase kinase 3 (GSK3), and Bad (20). Upon recruitment of Akt1 to the cell membrane, initiated by interactions of its pleckstrin homology (PH) domain with phosphoinositides, the 3-phosphoinositide–dependent kinase 1–dependent (PDK1-dependent) T308 phosphorylation in the activation T-loop is critical for Akt1 activation (23, 24). Subsequently, phosphorylation of S473 within a C-terminal hydrophobic motif of Akt1 occurs by mammalian target of rapamycin (mTOR), thereby determining substrate specificity of Akt1 (21, 25, 26). Fine tuning of Akt1 kinase activity also requires protein tyrosine phosphatases such as phosphatase and tensin homolog deleted on chromosome 10 (PTEN), which dephosphorylates phosphatidylinositol-(3,4,5)-trisphosphate (27), and protein phosphatase 1 (PP1) and PP2A (28, 29), which directly dephosphorylate Akt1. PTEN, PP1, and PP2A are ubiquitously expressed and can bind and regulate a large number of different proteins. For example, PP1 contributes to β_1 integrin/β_3 integrin interactions (30), and its activity is induced by ionizing radiation in a manner dependent on ataxia telangiectasia mutated (ATM; ref. 31). Many of these proteins recruit PP1 through a hydrophobic consensus motif, termed *PP1-binding site*, which consists of a RVXF binding groove (29, 32).

Authorship note: Iris Eke and Ulrike Koch contributed equally to this work.

Conflict of interest: The authors have declared that no conflict of interest exists.

Citation for this article: *J Clin Invest.* 2010;120(7):2516–2527. doi:10.1172/JCI41078.

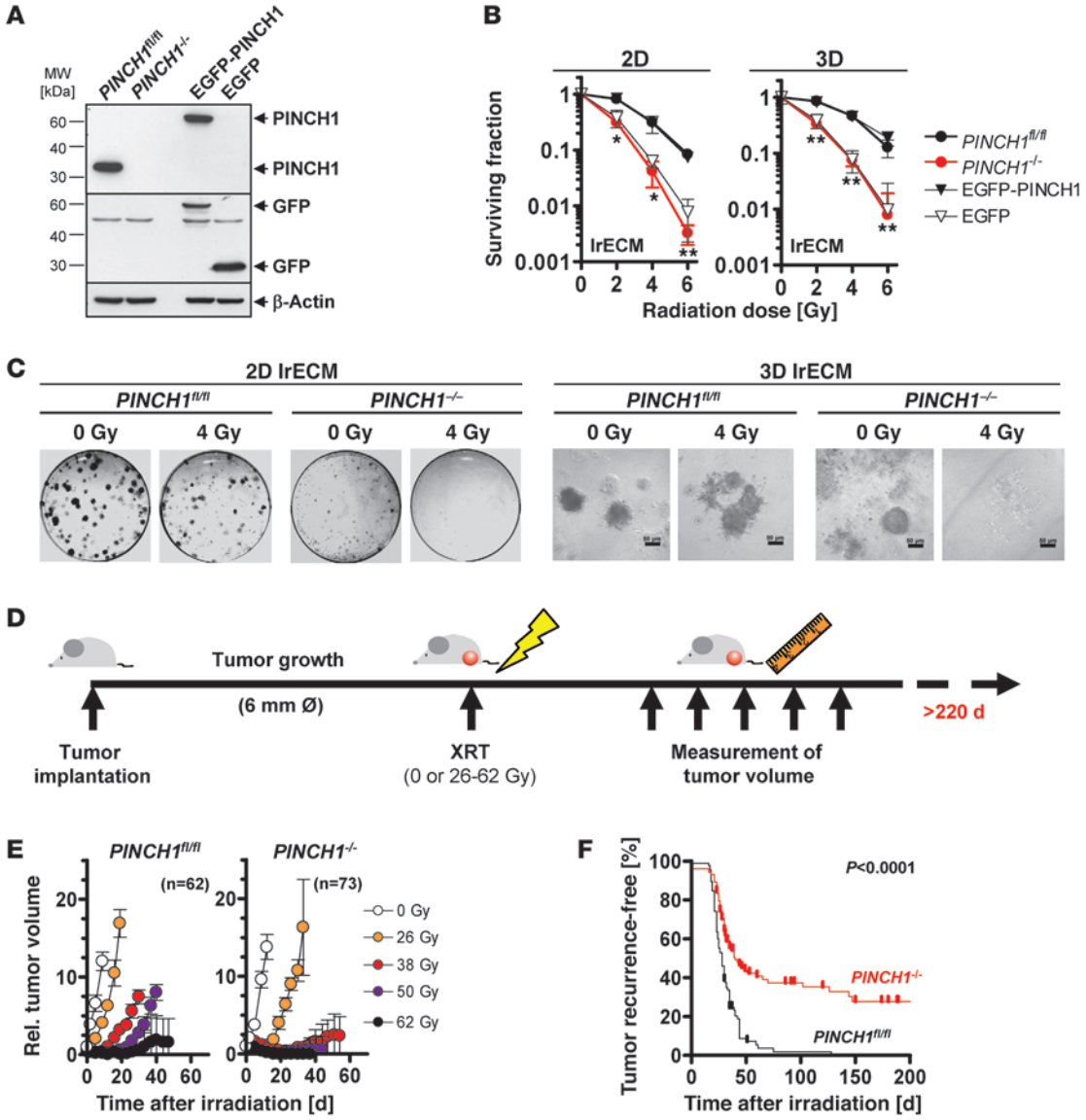

Figure 1

PINCH1 determines cellular sensitivity to ionizing radiation in vitro and in vivo. (**A**) Western blot analysis of PINCH1, EGFP-PINCH1, and EGFP expression in MEFs. β-Actin served as loading control. (**B**) Mean ± SD results from 2D or 3D clonogenic survival assays of nonirradiated or irradiated (0–6 Gy X-rays) IrECM cell cultures ($n = 3$; $^*P < 0.05$, $^{**}P < 0.01$, t test). (**C**) Representative images of 2D and 3D IrECM colony formation of nonirradiated or irradiated *PINCH1*$^{fl/fl}$ and *PINCH1*$^{-/-}$ MEF cultures at 11 days after plating. Scale bars: 50 μm. (**D**) Experimental in vivo setup. Subcutaneous allograft *PINCH1*$^{fl/fl}$ and *PINCH1*$^{-/-}$ tumors were grown in immunocompromised mice. After tumor formation (diameter approximately 6 mm), tumors were locally irradiated with increasing single doses of 26–62 Gy under homogeneous hypoxia (200 kV X-rays, 0.5 mm copper filter, dose rate approximately 1.3 Gy/min). Tumor volume was measured over a time period of 210 days after irradiation. (**E** and **F**) Volume of *PINCH1*$^{fl/fl}$ and *PINCH1*$^{-/-}$ allograft tumors in immunocompromised mice plotted against time after irradiation (mean ± SEM; $n = 10$–18 per group), and tumor recurrence–free survival of *PINCH1*$^{fl/fl}$ and *PINCH1*$^{-/-}$ tumor-bearing mice (Kaplan-Meier statistics and log-rank test) after irradiation (see also Supplemental Figure 3).

In the present study, we evaluated whether there is a link between the prosurvival factors PINCH1 and Akt1 for regulating radioresistance. We found that PINCH1 was overexpressed in human tumors and was essentially contributing to radiation cell survival in vitro and in vivo. Mechanistically, this PINCH1 function was mediated by direct interaction of PINCH1 and PP1α through a KFVEF binding motif at the LIM5 domain of PINCH1. The binding of PP1α by PINCH1 inhibited PP1α activity, causing Akt1 phosphorylation and radioresistance.

Results

PINCH1 is a critical regulator of cellular sensitivity to ionizing radiation and cytotoxic drugs. To examine how PINCH1 affects cell survival upon irradiation, we exposed mouse embryonic fibroblasts (MEFs) lacking PINCH1 expression (*PINCH1*$^{-/-}$ MEFs; Figure 1A) to ionizing radiation and found in colony formation assays that they showed significantly enhanced sensitivity to irradiation compared with *PINCH1*$^{fl/fl}$ MEFs (Figure 1, A–C). Similar results were obtained when cells were grown on 2D or 3D

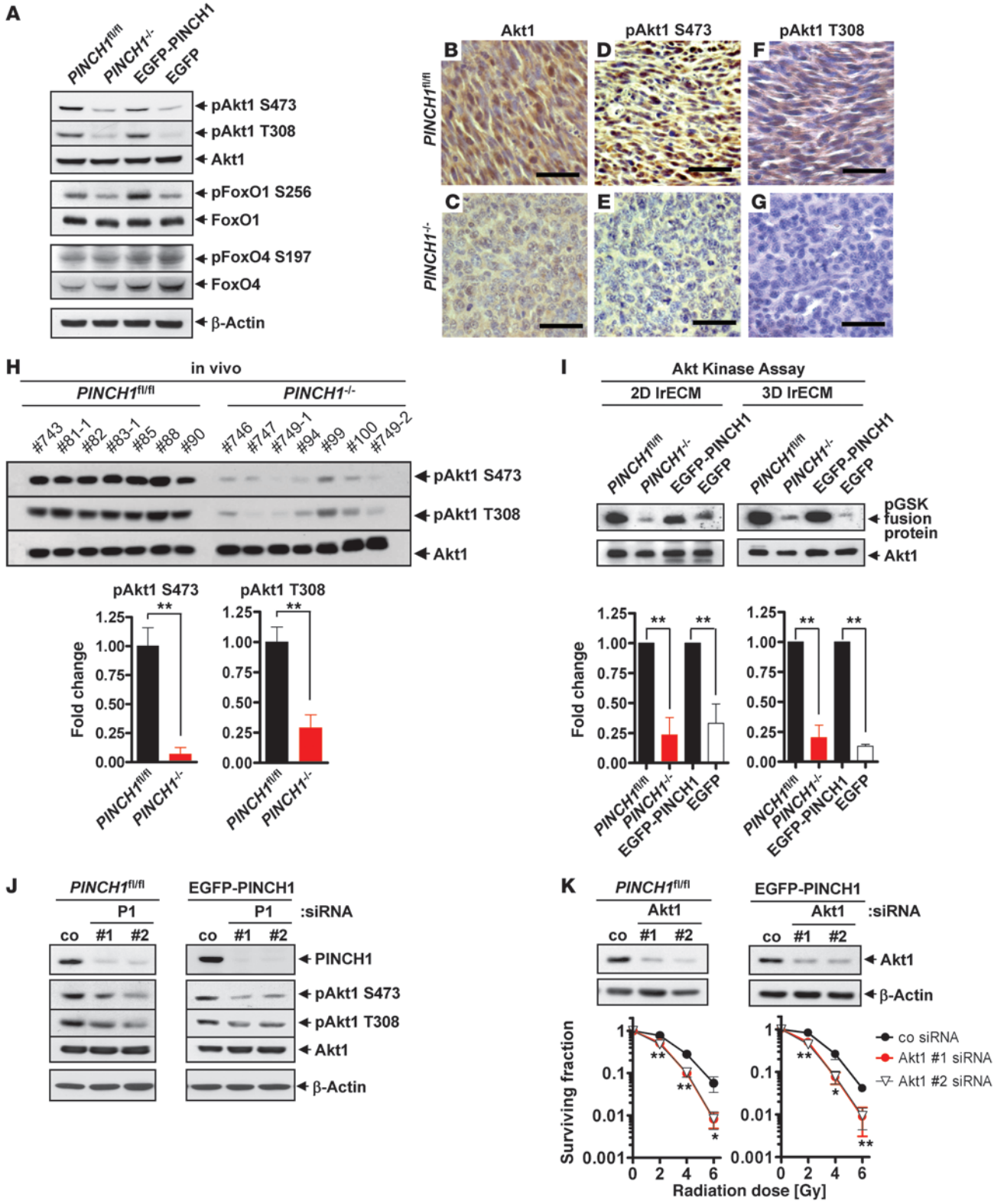
A
PINCH1fl/fl
PINCH1-/-
EGFP-PINCH1
EGFP
pAkt1 S473
pAkt1 T308
Akt1
pFoxO1 S256
FoxO1
pFoxO4 S197
FoxO4
β-Actin
Akt1
pAkt1 S473
pAkt1 T308
B
D
F
C
E
G
PINCH1fl/fl
PINCH1-/-
H
in vivo
PINCH1fl/fl
PINCH1-/-
#743
#81-1
#82
#83-1
#85
#88
#90
#746
#747
#749-1
#94
#99
#100
#749-2
pAkt1 S473
pAkt1 T308
Akt1
pAkt1 S473
pAkt1 T308
Fold change
1.25
1.00
0.75
0.50
0.25
0.00
**
PINCH1fl/fl
PINCH1-/-
I
Akt Kinase Assay
2D lrECM
3D lrECM
PINCH1fl/fl
PINCH1-/-
EGFP-PINCH1
EGFP
pGSK fusion protein
Akt1
Fold change
**
PINCH1fl/fl
PINCH1-/-
EGFP-PINCH1
EGFP
J
PINCH1fl/fl
EGFP-PINCH1
P1
:siRNA
co
#1
#2
PINCH1
pAkt1 S473
pAkt1 T308
Akt1
β-Actin
K
PINCH1fl/fl
EGFP-PINCH1
Akt1
:siRNA
co
#1
#2
Akt1
β-Actin
Surviving fraction
1
0.1
0.01
0.001
0
2
4
6
**
*
co siRNA
Akt1 #1 siRNA
Akt1 #2 siRNA
Radiation dose [Gy]

Figure 2
PINCH1 is critical for Akt1 phosphorylation and kinase activity. (**A**) Western blotting for total and phosphorylated amounts of Akt1, FoxO1, and FoxO4. β-Actin served as loading control (see also Supplemental Figure 5). (**B**–**G**) Immunohistochemistry for total (**B** and **C**) or S473 (**D** and **E**) or T308 (**F** and **G**) phosphorylated Akt1 in *PINCH1*$^{fl/fl}$ and *PINCH1*$^{-/-}$ allografts. Representative images are shown. Scale bars: 50 μm. (**H**) Western blot analysis of total and phosphorylated amounts of Akt1 (S473, T308) in protein lysates of *PINCH1*$^{fl/fl}$ and *PINCH1*$^{-/-}$ allografts tumors (#, animal no.). Fold changes were calculated from densitometric analysis of protein bands of S473 or T308 phosphorylated Akt1 (mean ± SD; $n = 7$; $^{**}P < 0.01$, *t* test). (**I**) Western blot analysis of Akt1 kinase assay using Akt1 immunoprecipitates from 2D and 3D lrECM cell cultures. Fold changes were calculated from densitometric analysis of protein bands of phosphorylated GSK fusion protein (mean ± SD; $n = 3$; $^{**}P < 0.01$, *t* test). (**J**) siRNA-mediated PINCH1 (P1) knockdown in *PINCH1*$^{fl/fl}$ and EGFP-PINCH1 MEFs and Western blot analysis of total and phosphorylated amounts of Akt1 (S473, T308). co, nonspecific siRNA control. (**K**) siRNAs targeting Akt1 in unirradiated or irradiated (0–6 Gy) *PINCH1*$^{fl/fl}$ and EGFP-PINCH1 MEF for clonogenic survival (mean ± SD; $n = 3$; $^{*}P < 0.05$, $^{**}P < 0.01$, *t* test). siRNA-mediated Akt1 depletion was confirmed by Western blotting. β-Actin served as loading control.

laminin-rich, basement membrane–like ECM (lrECM; Figure 1, B and C). Furthermore, enhanced sensitivity to irradiation or to the chemotherapeutic cisplatin was seen when *PINCH1*$^{-/-}$ cells were grown on fibronectin (Supplemental Figure 1, A and B; supplemental material available online with this article; doi:10.1172/JCI41078DS1). Importantly, reexpression of EGFP-PINCH1 by retroviral transduction abolished the radiosensitization (Figure 1, A and B, and Supplemental Figure 1A).

To verify the PINCH1 knockout–dependent increase in radiosensitivity in vivo, allograft tumors of immortalized *PINCH1*$^{fl/fl}$ and *PINCH1*$^{-/-}$ cell lines were established in immunocompromised mice (Figure 1, D–F, and Supplemental Figure 2, A and B). When tumors reached a diameter of 6 mm, they were irradiated with increasing single doses of X-rays (26–62 Gy) and monitored up to 210 days. Consistent with the in vitro results, *PINCH1*$^{-/-}$ allografts demonstrated significantly higher radiosensitivity than did *PINCH1*$^{fl/fl}$ allografts in terms of both tumor growth delay and tumor recurrence–free survival (Figure 1, E and F, Supplemental Figure 3, A–C, and Supplemental Tables 1 and 2). Moreover, *PINCH1*$^{fl/fl}$ tumors exhibited a different morphology and grew faster, as indicated by volume measurement and Ki-67 labeling index, than did *PINCH1*$^{-/-}$ tumors (Supplemental Table 2 and Supplemental Figure 4, A–C).

The sensitivity of tumors to radiation can be substantially reduced by microenvironmental factors such as hypoxia (33). Therefore, we examined hypoxia, necrosis, and vascularization in *PINCH1*$^{fl/fl}$ and *PINCH1*$^{-/-}$ tumors by injecting the hypoxia marker pimonidazole and Hoechst 33342 and then staining for the endothelial cell marker CD31. Interestingly, no significant differences for hypoxia, necrosis, and vascularization were found between *PINCH1*$^{fl/fl}$ and *PINCH1*$^{-/-}$ tumors (Supplemental Figure 4, A, D, and E).

Akt1 phosphorylation and kinase activity critically depend on PINCH1. To define the signaling cascades responsible for PINCH1-dependent regulation of radiation survival, we examined the prosurvival protein kinase Akt1 (21). Consistent with compromised survival upon irradiation, *PINCH1*$^{-/-}$ cells and *PINCH1*$^{-/-}$ allografts showed reduced levels of phosphorylated S473 and T308 of Akt1 compared with *PINCH1*$^{fl/fl}$ cells, *PINCH1*$^{fl/fl}$ allografts, and PINCH1 knockout MEFs reconstituted with EGFP-PINCH1 (Figure 2, A–H, and Supplemental Figure 5A). The reduced Akt1 activity was also reflected by significantly decreased phosphorylation of FoxO1 at S256, whereas other Akt1 interacting proteins, such as FoxO4 and GSK3β (Supplemental Figure 5B and ref. 21), remained unchanged.

To verify changes in Akt1 activity, Akt1 kinase activity was measured in Akt1 immunoprecipitates from 2D and 3D lrECM cell cultures and found to be significantly reduced both in monolayer and in 3D cell cultures upon PINCH1 deletion (Figure 2I). To test the robustness of the PINCH1/Akt1 interrelation, we next examined changes in Akt1 phosphorylation upon siRNA-mediated PINCH1 knockdown and measured clonogenic survival of *PINCH1*$^{fl/fl}$ and EGFP-PINCH1 cells after Akt1 siRNA knockdown and irradiation. Strikingly, PINCH1 knockdown caused a strong reduction of Akt1 S473 and T308 phosphorylation (Figure 2J), and Akt1 knockdown significantly enhanced the radiosensitivity of PINCH1-expressing MEFs (Figure 2K). Taken together, these data suggest that PINCH1 is critical for radiation survival and Akt1 phosphorylation and activity.

PINCH1 mRNA and protein expression in human tumors. To determine whether PINCH1 also plays a role in human tumors, we investigated its mRNA expression in selected tumor entities and corresponding normal tissues using Oncomine data sets as well as its protein expression in biopsies from patients with colorectal carcinoma. Importantly, comparison of PINCH1 transcriptomic profiles from tumor versus normal tissues from the most frequent tumor entities worldwide, such as lung, colon, breast, and prostate, showed a highly significant increase in mRNA expression in the tumors (Figure 3A and Supplemental Table 3). Moreover, biopsies of colorectal carcinomas (Figure 3B) also revealed a highly significant elevation of PINCH1 protein expression compared with normal colon.

Radiation survival is controlled by Akt1 S473 phosphorylation in a PINCH1-dependent manner. To confirm the role of PINCH1 in regulating resistance to radiation by interacting with Akt1, we next depleted PINCH1 in human cancer cell lines originating from colon (DLD1, HCT15, and HCT116), lung (A549 and H1299), cervix (Hela), skin (A431), and pancreas (PaTu and MiaPaCa2). In perfect agreement with our findings using MEFs, all carcinoma cell lines showed significant radiosensitization after siRNA-mediated PINCH1 depletion compared with cells treated with nonspecific siRNA controls (Figure 3C and Supplemental Figure 6A). Similarly, PINCH1-depleted cancer cell lines exhibited significant chemosensitization to cisplatin, gemcitabine, and 5-fluorouracil (5-FU; Figure 3D and Supplemental Figure 6, B and C). Furthermore, PINCH1 depletion resulted in a striking reduction of the phosphorylation of Akt1 (S473 and T308), FoxO1 (S256), and FoxO4 (S197), but not GSK3β, relative to siRNA controls (Figure 3E and Supplemental Figure 7, A–C). Thus, PINCH1 crucially determines Akt1 phosphorylation and radiation survival in mammalian cells with varying genetic backgrounds.

To further define whether the effects of PINCH1 are linked with Akt1, we evaluated the impact of single Akt1 versus combined Akt1/PINCH1 knockdown in DLD1 cells. Single Akt1 knockdown significantly reduced the radiation survival of DLD1 cells (Figure 4A). Combined Akt1/PINCH1 knockdown resulted in survival that was superimposable to that obtained with single Akt1 knockdown (Figure 4A). These data indicate that PINCH1 and Akt1 act in the same signaling pathway.

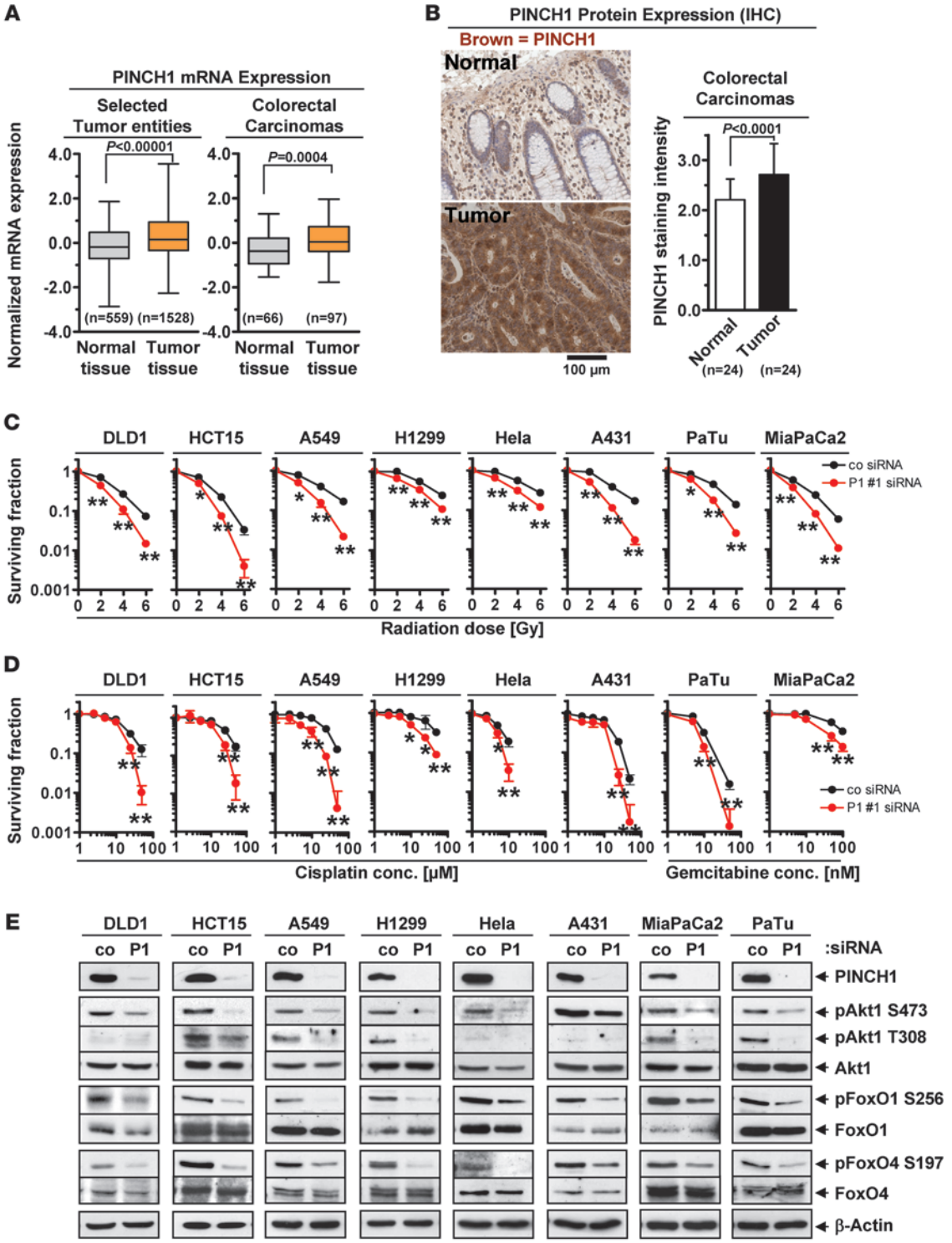

Figure 3

PINCH1 mRNA and protein expression in colorectal carcinoma and effects of PINCH1 depletion in human carcinoma cell lines. (**A**) Analysis of PINCH1 mRNA expression in normal and tumor tissues from Oncomine data sets. List of tumor entities is displayed in Supplemental Table 3. Colorectal carcinomas have been analyzed selectively. (**B**) PINCH1 protein expression in biopsies of human colorectal carcinomas. Columns show mean PINCH1 staining intensities and statistical analysis including tumor grading 2 to 4 (mean ± SD; $n = 24$; χ^2 test). Scale bar: 100 µm. (**C** and **D**) Clonogenic survival was measured in irradiated (0–6 Gy X-rays) (**C**) or 1 hour cisplatin- or 24 hours gemcitabine-treated (**D**) human colorectal (DLD1, HCT15), lung (A549, H1299), cervix (Hela), skin (A431), and pancreatic (PaTu, MiaPaCa2) carcinoma cell lines under PINCH1 knockdown. Data are mean ± SD ($n = 3$; $^{**}P < 0.01$, t test). (**E**) PINCH1 knockdown cultures of human cancer cell lines were examined for total and phosphorylated amounts of the indicated proteins. P1, PINCH1.

How does PINCH1 regulate Akt1 phosphorylation and kinase activity? We hypothesized that PINCH1 regulates either the phosphorylation of specific sites of Akt1, i.e., S473 or T308, or membrane translocation of Akt1, i.e., through its PH domain (21, 34). To distinguish between the 2 possibilities, we transiently transfected PINCH1-depleted human DLD1 colorectal carcinoma cells with different RFP-Akt1 plasmids (35) and assayed clonogenic survival and Akt1 phosphorylation. Strikingly, on a PINCH1 knockdown background, neither Akt1 mutants expressing single S→A kinase function–disrupting substitution at residue 473 (S473A) nor mutants expressing double kinase function–disrupting substitution of S→A plus T→A at residue 473 and 308 (S473A/T308A) were able to revert clonogenic radiation survival levels to that of Akt1 WT (Figure 4, B and C). Additionally, both the constitutive active Akt1 mutant (S→D plus T→D at residues 473 and 308 [S473D/T308D]) as well as the deletion mutant of the aminoterminal PH domain of Akt1 (Akt1ΔPH) mediated radiation survival in the absence of PINCH1 in a manner similar to that observed for Akt1 WT (Figure 4, B and C). The coincidence of similarity in radiation survival mediated by Akt1 WT, S473D/T308D, and Akt1ΔPH on a PINCH1 knockdown background and presence of phosphorylated Akt1 S473 (Figure 4, B and C) indicate that the S473 phosphorylation site is the essential site for Akt1 regulation of radiation survival by PINCH1. Moreover, the retained ability of the Akt1ΔPH construct to rescue radiation survival of PINCH1-depleted DLD1 cells suggests that translocation of Akt1 to the cell membrane is not required for its prosurvival signaling. In the presence of PINCH1, DLD1 radiation survival remained unaltered by all tested Akt1 plasmids (Figure 4C). Taken together, these findings demonstrate that Akt1 lies downstream of PINCH1 in survival signaling.

PINCH1 determines the activity of Akt1 through the recruitment of PP1α. To investigate whether PINCH1 and Akt1 interact physically, we performed mass spectrometry (MS) on EGFP and Akt1 immunoprecipitates from EGFP-PINCH1–reconstituted MEFs. The Akt1-regulating PP1α was detected in both EGFP-PINCH1 and Akt1 immunoprecipitates, identifying PP1α as a potential PINCH1-to-Akt1 linker protein (Supplemental Table 4). It has previously been shown that PP1α can control Akt1 activity (28), although the underlying regulatory mechanism is still unclear.

Next, we examined whether PINCH1, Akt1, and PP1α colocalize in cells and how loss of PINCH1 affects PP1α phosphatase activity. Interestingly, both Akt1 and PP1α were found together with EGFP-PINCH1 in FAs (Supplemental Figure 8). Moreover, loss of PINCH1 expression caused significantly elevated PP1α phosphatase activity without affecting the PP1α protein levels (Figure 5A and Supplemental Figure 9, A and B). Similarly, DLD1 cells also exhibited significantly increased phosphatase activity upon PINCH1 knockdown (Figure 5B and Supplemental Figure 9C). Finally, 2 nonspecific phosphatase inhibitors, okadaic acid (36) and tautomycetin (37), efficiently reduced the activity of PP1α in *PINCH1*$^{fl/fl}$ MEFs (Figure 5A). These data suggest that PINCH1 binds and regulates the phosphatase activity of PP1α.

Binding of PP1α to PINCH1 via a KFVEF motif controls Akt1 phosphorylation and radiation survival. To identify the PP1α binding motif of PINCH1, we analyzed the primary sequence of PINCH1 and found a highly conserved putative PP1α binding motif (32), KFVEF, at the aminoterminal PINCH1-LIM5 domain (Figure 5C). EGFP-PINCH1 without the LIM5 domain or point mutations in the KFVEF site (double V→A plus F→A substitution at residues 304 and 306 [V304A/F306A]; triple K→A plus V→A plus F→A substitution at residues 302, 304, and 306 [K302A/V304A/F306A]) were expressed in *PINCH1*$^{-/-}$ MEFs (Figure 5D) and failed to coprecipitate PP1α (Figure 5E). This indicates that the LIM5 domain with an intact KFVEF motif is required for an efficient PINCH1/PP1α interaction. As a consequence of the severely reduced PINCH1/PP1α association by deletion or mutation of the KFVEF motif, PP1 phosphatase activity remained elevated (Figure 5F), and Akt1 phosphorylation decreased (Figure 6A), compared with *PINCH1*$^{-/-}$ MEFs expressing EGFP-PINCH1 WT.

Although it has recently been shown that ILK is a pseudokinase (38), we excluded the PINCH1 binding partner ILK as a potential S473 kinase (19). In whole-cell lysates, we found reduced ILK expression levels in *PINCH1*$^{-/-}$ EGFP controls, but normal ILK expression in *PINCH1*$^{-/-}$ MEFs expressing EGFP-PINCH1 WT, EGFP-PINCH1ΔLIM5, or mutated KFVEF motifs (Figure 6A). These findings confirmed the interdependence of ILK expression and PINCH1 (39). Furthermore, ILK colocalized with PINCH1 WT and PINCH1 mutants in FAs (Figure 6B), whereas ILK was not in FAs of *PINCH1*$^{-/-}$ MEFs (data not shown). Taken together, these results suggest that PINCH1 regulates Akt1 through PP1α in an ILK-independent manner. As a consequence of an impeded PINCH1/PP1α interaction, the cellular radiosensitivity of *PINCH1*$^{-/-}$ MEFs expressing EGFP, EGFP-PINCH1ΔLIM5, or mutated KFVEF motifs was significantly enhanced at the clinically relevant radiation dose per fraction of 2 Gy compared with EGFP-PINCH1 WT–expressing MEFs (Figure 6C).

Discussion

Here, we showed that mRNA and protein expression of the FA adapter protein PINCH1 were significantly increased in human tumors of diverse origin, particularly colorectal carcinoma; that PINCH1 was critical for the regulation of cellular radio- and chemosensitivity; and that this function was mediated through the binding of PP1α to the KFVEF motif within the LIM5 domain, which caused inhibition of PP1α, activation of its downstream target Akt1, and, finally, enhanced radiation cell survival.

PINCH1 essentially contributes to cellular resistance to radio- and chemotherapy. The combination of surgery and chemo- and radiotherapy leads to cancer cure rates greater than 50% among all cancer types. Limitations for further increases of these cure rates predominantly arise from normal tissue radiosensitivity and from dose-limiting, chemotherapy-related side effects. Therefore, the identification of key molecules acting in the survival pathways of tumor cells may allow the development of potent targeted strategies reducing tumor cell resistance to radio- and chemotherapy. Although it is well accepted that integrin-mediated adhesion promotes tumor cell resistance, it is less well understood how integrins execute this prosurvival effect in cancer cells. We report here that loss of PINCH1, which acts downstream of integrins, dramatically diminished clonogenic radiation cell survival and reduced cellular resistance to cisplatin, gemcitabine, and 5-FU. These profound effects were observed in *PINCH1*$^{-/-}$ MEFs and PINCH1-depleted human carcinoma cell lines originating from colon, lung, cervix, skin, and pancreas and confirmed in the MEF tumor xenograft model by measurement of tumor recurrence–free survival. Considering the administration of high, clinically irrelevant radiation doses in this study, examination of tumor recurrence under clinically more relevant fractionated radiation regimes in PINCH1-depleted human tumor models is warranted to support our notion of PINCH1 as putative cancer target. It is well known that cellular radiosensitivity can be substantially

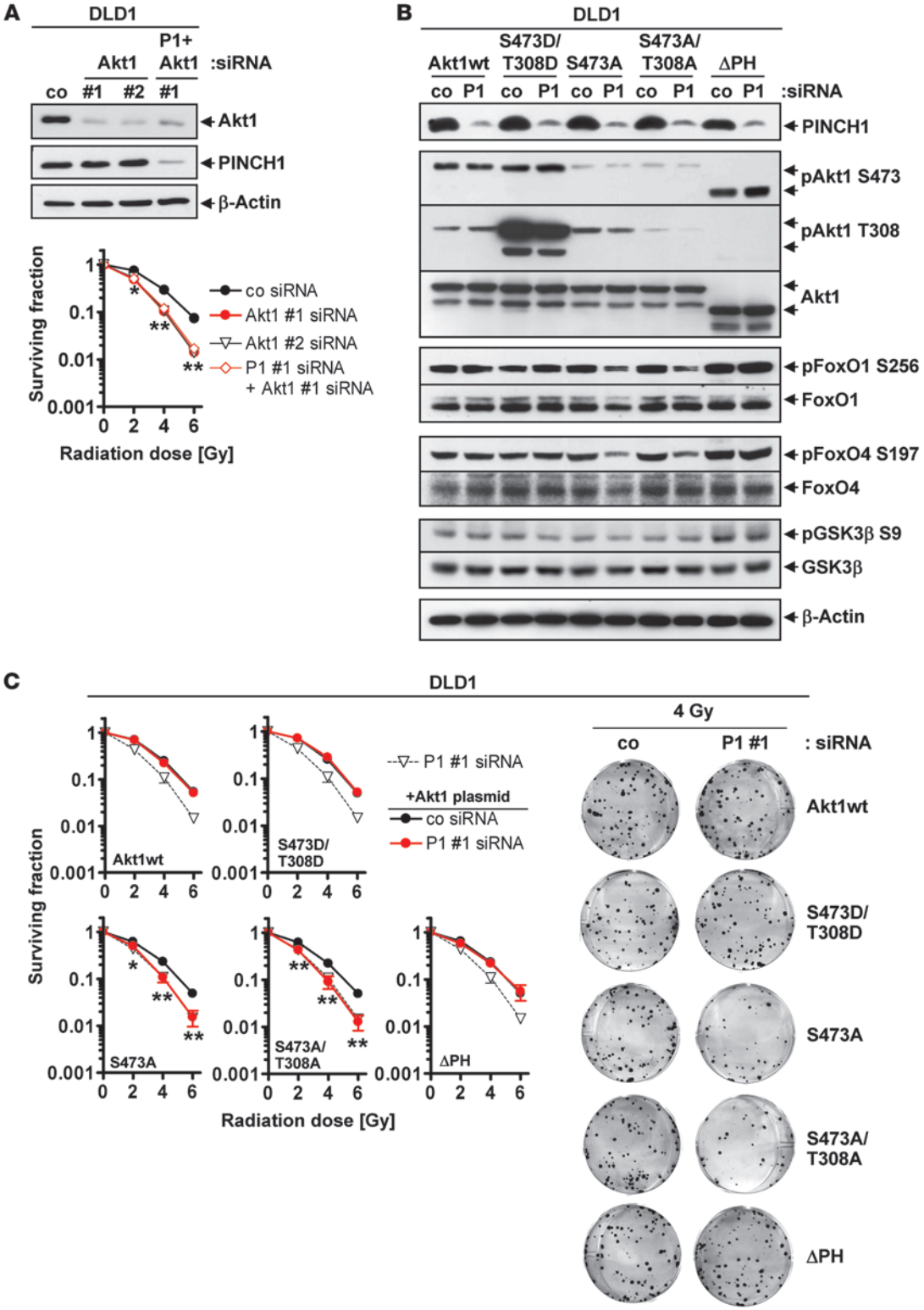

Figure 4

Phosphorylated S473 of Akt1 determines PINCH1-dependent radiation survival. (**A**) Western blot analysis of Akt1 and PINCH1 upon single or combined siRNA-mediated Akt1 and PINCH1 knockdown in DLD1 cells. Radiation survival of DLD1 PINCH1 knockdown cells was determined upon Akt1 siRNA knockdown (mean ± SD; $n = 3$; $^*P < 0.05$, $^{**}P < 0.01$, *t* test). (**B**) Total and phosphorylated amounts of exogenous RFP-Akt1 (WT, S473D/T308D, S473A, S473A/T308A or ΔPH) and associated signaling molecules were evaluated in DLD1 PINCH1 knockdown cultures by Western blotting. (**C**) Clonogenic radiation survival (0–6 Gy X-rays) was measured in DLD1 PINCH1 knockdown cultures transiently transfected with RFP-Akt1 plasmids expressing WT, S473D/T308D, S473A, S473A/T308A, or ΔPH (mean ± SD; $n = 3$; $^*P < 0.05$, $^{**}P < 0.01$, *t* test). Representative images demonstrate colony formation under tested experimental conditions.

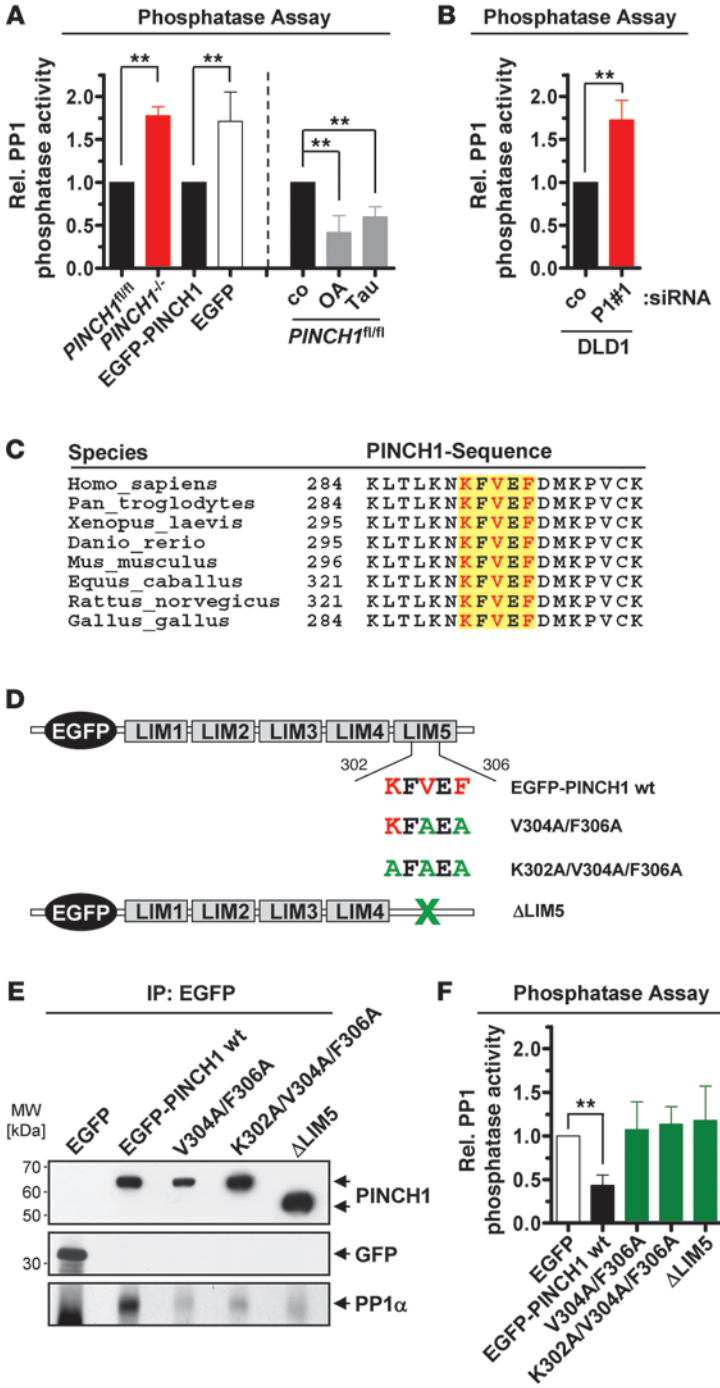

Figure 5

PINCH1 interacts with PP1α to regulate Akt1 phosphorylation. (**A**) Protein phosphatase activity from MEFs left untreated or treated with okadaic acid (OA) or tautomycetin (Tau). Data are mean ± SD ($n = 4$; $^{**}P < 0.01$, *t* test). (**B**) Protein phosphatase activity of PINCH1 knockdown DLD1 and control cultures. Data are mean ± SD ($n = 4$; $^{**}P < 0.01$, *t* test). (**C**) Sequence homology search for the putative binding sequence KFVEF. (**D**) Schematic of mouse PINCH1 WT, PINCH1 V304A/F306A, PINCH1 K302A/V304A/F306A, and PINCH1ΔLIM5 inserted into pEGFP-C1 vector. (**E** and **F**) EGFP immunoprecipitates from *PINCH1*$^{-/-}$ MEF transfected with EGFP, EGFP-PINCH1 WT, V304A/F306A or K302A/V304A/F306A mutated KFVEF motifs, or EGFP-PINCH1ΔLIM5 were examined for total amounts of indicated proteins and protein phosphatase activity (mean ± SD; $n = 3$; $^{**}P < 0.01$, *t* test).

modulated by the tumor micromilieu, for example through pathological blood vessels or hypoxia (33, 40, 41). Since the tumor micromilieu was not affected by the loss of PINCH1, we conclude that the differences in tumor recurrence–free survival are tumor cell autonomous and predominantly PINCH1 dependent.

We and others have identified FA proteins that control tumor cell resistance. They include β_1 and β_3 integrins (4, 42, 43) as well as the EGFR (8, 9, 44), which acts together with integrins. These proteins were found to be overexpressed in diverse human malignancies. Interestingly, this was also the case for PINCH1, whose mRNA was significantly elevated compared with corresponding normal tissues. Furthermore, we found significantly increased levels of PINCH1 protein in colorectal carcinomas. Thus, the elevated PINCH1 levels in different cancers support our notion of PINCH1 serving as a potential cancer target.

PINCH1/PP1α interaction controls Akt1 phosphorylation. LIM-containing proteins such as PINCH1 serve as a platform for recruiting and regulating the activity of downstream signaling molecules, either by direct activation or inhibition of the enzymatic activity or by spatial localization (45). PINCH1 was shown to recruit a number of proteins, such as ILK and Nck2, that link integrin and growth factor receptor signaling. While the interaction with Nck2 at the PINCH1 LIM4 domain seems extremely weak (46), ILK binding to the LIM1 domain of PINCH1 is of high affinity and required for the stability and localization of the PINCH1/ILK/parvin complex to FAs (15, 39, 47). Furthermore, the PINCH1/ILK interaction triggers signaling cascades required for cell survival and proliferation (39, 47, 48). The underlying mechanism for these important tasks was initially ascribed to the catalytic activity of ILK (49). It has been suggested that ILK controls cell proliferation by altering the activity of GSK3β or of specific prosurvival signal transduction pathways, such as the PI3K/Akt1 axis, which also play essential roles in radioresistance (22, 50). As a large number of genetic studies in flies, worms, and mice clearly showed that ILK is a pseudokinase (13, 24, 38), we sought for a mechanistic explanation of how PINCH1 regulates the activity of Akt1 and, consequently, radioresistance of tumor cells.

Since simultaneous PINCH1/Akt1 depletion caused radiation cell survival similar to that of single depletion of each of these proteins alone, we hypothesized that these 2 proteins act in the same signaling cascade. Given that overexpression of WT Akt1, constitutively active Akt1, and Akt1ΔPH rescued radiation survival of PINCH1-depleted tumor cells, and kinase function–disrupting mutations at S473 and S473/T308 failed to do so, we concluded that clonogenic survival of irradiated cells critically depends on the phosphorylation of Akt1. The PH domain of Akt1 seems not to be required to abolish PINCH1 knockdown–mediated radiosensitization. This finding could be explained by a possible prosurvival communication between PINCH1 and Akt1ΔPH distant from the cell membrane.

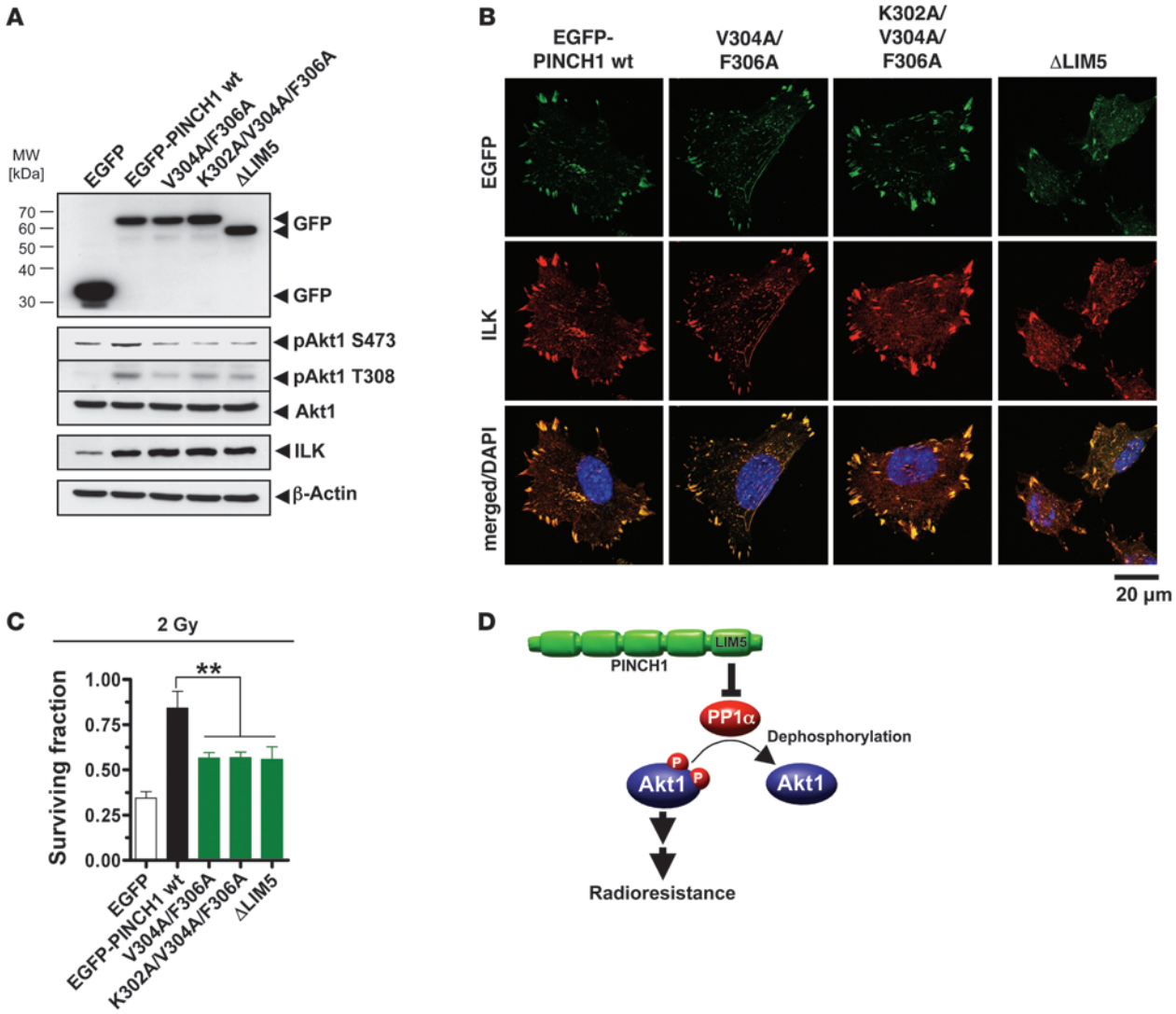

Figure 6

PINCH1 regulates cellular radiation survival by PP1α-dependent inhibition of Akt1. (**A**) Western blot of EGFP, Akt1 (S473, T308) and ILK from *PINCH1*$^{-/-}$ MEF transfected with EGFP, EGFP-PINCH1 WT, V304A/F306A or K302A/V304A/F306A mutated KFVEF motifs, or EGFP-PINCH1ΔLIM5. β-Actin served as loading control. (**B**) Confocal fluorescence images on the subcellular localization of the different PINCH1 mutants described in **A** and of the putative Akt1 S473 phosphorylator ILK. Scale bar: 20 μm. (**C**) Clonogenic radiation survival of 2 Gy–irradiated *PINCH1*$^{-/-}$ MEF transfected with EGFP, EGFP-PINCH1 WT, V304A/F306A or K302A/V304A/F306A mutated KFVEF motifs, or EGFP-PINCH1ΔLIM5. Data are mean ± SD (n = 3; $^{**}P < 0.01$, t test). (**D**) Proposed mechanisms how PINCH1 interacts with PP1α via the LIM5 domain of PINCH1. This interaction inhibits Akt1 dephosphorylation and contributes to cellular radioresistance.

To unravel the cooperation between PINCH1 and Akt1, we precipitated PINCH1 and Akt1, respectively, and determined their interactomes by MS. In both PINCH1 and Akt1 precipitates, we found the Akt1-regulating PP1α. A sequence homology search revealed a single highly conserved PP1α binding motif, KFVEF, in the LIM5 domain of PINCH1. In immunoprecipitates from *PINCH1*$^{-/-}$ MEFs expressing LIM5 domain–deleted PINCH1 or PINCH1 with point mutations in the KFVEF motif (i.e., V304A/F306A and K302A/V304A/F306A), PP1α was absent, thus confirming the high relevance of this particular binding sequence for PP1α binding to PINCH1. When PP1α was properly bound to PINCH1 through the KFVEF motif at the PINCH1 LIM5 domain, PP1α phosphatase activity was inhibited. Intriguingly, this PP1α inhibition effectively prevented dephosphorylation of Akt1 at S473 and T308 and enhanced cellular resistance to ionizing radiation. With regard to the pseudokinase ILK and its requirement for proper signaling together with PINCH1, we examined ILK protein expression and FA localization in *PINCH1*$^{-/-}$ MEFs expressing WT PINCH1, PINCH1ΔLIM5, or KFVEF mutants. Although the expression of PINCH1 mutants rescued total ILK expression and subcellular localization to FAs, the PINCH1 mutants were unable to restore Akt1 S473 phosphorylation and PP1α functionality. Despite these molecular observations, the expression of PINCH1 mutants caused higher radiation survival compared with EGFP controls, indicating additional, yet to be defined prosurvival signals. Therefore, it remains to be determined which function the structural interaction between PINCH1 and ILK

plays for PP1α binding. Our findings demonstrate a mode of action for how PINCH1 and PP1α interact to regulate Akt1 phosphorylation and cellular radioresistance, which we believe to be novel.

In summary, our data showed PINCH1 overexpression in various human tumors and defined what we believe to be a novel function of the LIM-only, FA-associated adapter protein PINCH1 in the cellular sensitivity to ionizing radiation in vitro and in vivo. The identification of stimulatory signals from PINCH1 to the prosurvival protein kinase Akt1 via PP1α delineates a mechanistic connection by which FA-associated processes essentially contribute to the regulation of the radiation survival response (Figure 6D). On the basis of PINCH1 overexpression in human malignancies, targeting PINCH1 represents a promising new therapeutic concept to overcome radio- and chemoresistance of tumor cells and to improve cure rates of cancer patients.

Methods

Cell culture, radiation exposure, and 2D and 3D colony formation assay. *PINCH1*$^{fl/fl}$ and *PINCH1*$^{-/-}$ MEFs and EGFP and EGFP-tagged full-length PINCH1 (EGFP-PINCH1) expressing PINCH1-deficient fibroblasts were generated as previously described (47). Human DLD1, HCT15, and HCT116 (colorectal adenocarcinoma); A549 and H1299 (lung carcinoma); Hela (cervical carcinoma); A431 (skin); and PaTu and MiaPaCa2 (pancreatic adenocarcinoma) cell lines were from ATCC. Single doses of 200 kV X-rays were applied. Treatment with cisplatin (0–50 μM; Neocorp), gemcitabine (Lilly), or 5-FU (0–250 μM; Medac) was performed for 1 hour followed by washing 3 times using PBS. Clonogenic survival was determined in 2D and 3D cell cultures as described in Supplemental Methods and as previously published (51).

Total protein extracts and Western blotting. Cell lysis, SDS-PAGE, Western blotting, and protein detection were performed as previously described (52).

Akt1 and PINCH1 expression constructs and site-directed mutagenesis. Akt1 plasmids were generated as described previously (35). The mouse PINCH1 WT and PINCH1 LIM5 deletion mutant (PINCH1ΔLIM5) were generated by PCR-based amplification with specific primers. Constructs were flanked with *Kpn*I and *Bam*HI restriction sites and inserted into the *Kpn*I and *Bam*HI sites of pEGFP-C1 (Clontech). Mutation of the KFVEF motif was performed using appropriate primers (see Supplemental Methods) and the QuikChange II Site-Directed Mutagenesis Kit (Stratagene) according to the manufacturer's instructions and confirmed by sequencing.

MS. In-gel digestion, LC-MS/MS analysis on the LTQ ion trap mass spectrometer (Thermo Fisher Scientific), and spectra processing procedure were performed on anti-GFP and anti-Akt1 antibody pulldowns from EGFP-PINCH1 MEFs as described previously (53). Proteins were identified in the mouse International Protein Index database (http://www.ebi.ac.uk/IPI; accessed April 2008) by MASCOT version 2.1 software (Matrix Science Ltd.). Protein hits were considered confident when at least 2 MS/MS spectra matched the corresponding database sequences with peptide ion scores exceeding the confidence threshold suggested by MASCOT ($P < 0.05$).

PP1 assay. To measure PP1 activity, the ProFluor Ser/Thr Phosphatase Assay kit (Promega) was used as described previously (54). Okadaic acid and tautomycetin were from Applichem and Tocris, respectively.

Mice and in vivo experiments. Animal facilities and experiments were approved by the Animal Care and Use Committee of the Medical Faculty Carl Gustav Carus, Dresden University of Technology, and the Regierungspräsidium Dresden according to the German animal welfare regulations. Immunocompromised 7- to 14-week-old male and female NMRI (nu/nu) mice were further immunosuppressed by whole-body irradiation 1–5 days before tumor transplantation. We serially transplanted cryopreserved chunks of *PINCH1*$^{fl/fl}$ and *PINCH1*$^{-/-}$ tumors onto the back of mice. For the experiments, pieces of approximately 1 mm size of second- and third-passage tumors with median growth rate were subcutaneously transplanted onto the right hind leg. PCR genotyping and PINCH1 protein expression of tumors was performed as described in Supplemental Methods. After reaching a tumor volume of 0.10–0.32 cm^3, animals were randomly allocated to the different radiation dose levels in groups of 4 animals. Single doses of 26, 32, 38, 44, 50, 56, or 62 Gy (200 kV X-rays) were given under homogeneous hypoxia using a heavy clamp placed over the proximal thigh of the tumor-bearing leg of anesthetized mice (120 mg/kg body weight ketamine i.p. and 16 mg/kg xylazine i.p.) 2 minutes before and during irradiation. *PINCH1*$^{fl/fl}$ and *PINCH1*$^{-/-}$ tumors were equally distributed over the dose groups (Supplemental Table 1).

Tumor volume, tumor growth delay, local tumor control, histology, and Western blotting. The tumor diameter was measured twice per week using a caliper. Tumor volumes were determined by the formula of a rotational ellipsoid: $\pi/6 \times a \times b^2$, where a is the longest and b is the perpendicular shorter tumor axis. Tumor growth time (TGT) of unirradiated and irradiated *PINCH1*$^{fl/fl}$ and *PINCH1*$^{-/-}$ tumors was evaluated from growth curves of individual tumors as the time needed after start of the experiment to reach 2 and 5 times the starting volume (TGT_{V2} and TGT_{V5}, respectively). Tumor volume was measured until tumors reached a volume of about 1.5 cm^3. Local tumor recurrences after irradiation were scored when the tumor volume increased for 3 consecutive measurements after passing a nadir. A total of 85 *PINCH1*$^{fl/fl}$ and 99 *PINCH1*$^{-/-}$ tumors were evaluated for local tumor control. In *PINCH1*$^{fl/fl}$ and *PINCH1*$^{-/-}$ tumor-bearing animals, 95% of all recurrences were scored before days 51 and 102 after irradiation, respectively. The last recurrences occurred at days 128 and 147 for *PINCH1*$^{fl/fl}$ and *PINCH1*$^{-/-}$, respectively. Animals without recurrent tumors within the radiation field (i.e., with locally controlled tumors) were followed up until death. For analysis of local tumor control data, censored animals were taken into account as described in Supplemental Methods. For histology, a total of 12 *PINCH1*$^{fl/fl}$ and 9 *PINCH1*$^{-/-}$ tumors were subjected to histological analysis. Methods to assess vasculature, hypoxia, and perfusion on frozen sections and index for Ki-67 staining on paraffin-embedded tumors were performed as described in Supplemental Methods. For analysis of Akt1 expression and phosphorylation, pieces of *PINCH1*$^{fl/fl}$ and *PINCH1*$^{-/-}$ tumors were homogenized and lysed (25 mM Tris-HCl, 1.5 mM EGTA, 0.5 mM EDTA, 1% Triton X-100, 1 mM Na_3VO_4, and 1 mM sodium pyruvate) on ice and subjected to SDS-PAGE, Western blotting, and protein detection.

Microarray data sets. For the analysis of PINCH expression data, Oncomine (http://www.oncomine.org) was searched for studies comparing tumor with normal tissue containing probes for PINCH1 (selected studies are listed in Supplemental References). Within a given data set, the probe was selected that possessed the higher expression values. The normalized values of the individual data sets were combined and further analyzed. Since single data sets are split by tissue type at Oncomine, the sample identifier was used to eliminate duplicates. Expression values representing chronically inflamed tissues like chronic pancreatitis were purged from the data. For the highly diverse class of brain tumors, only glioblastomas were included. Gene expression differences were analyzed by 2-sided Student's *t* test using GraphPad Prism software version 4.03.

Tissue specimens, tissue microarray, and immunohistochemistry. Paraffin blocks of 24 human tissue specimens each from tumor and normal tissues were taken from the archive of the Institute of Pathology under approval of the local ethics committee of the Dresden University of Technology and with the patients' consent. Paraffin sections were stained with a monoclonal mouse anti-PINCH1 antibody (P-9371; Sigma-Aldrich) at a dilution of 1:300 in an autostainer 480 (Labvision) according to the manufacturer's instructions. Counterstaining was performed with hematoxylin. Staining intensities of the samples were evaluated by a pathologist and were semiquantitatively scored using a 4-tiered

score (staining intensities of 0, 1, 2, and 3) as described previously (55). Statistical analysis tested PINCH1 expression in tumor versus normal tissues using a χ^2 test. Negative control reactions yielded no staining confirming the specificity of the antibody recognition.

Statistics. Data are presented as mean ± SD or mean ± SEM. The level of significance was determined by unpaired, 2-sided Student's *t* test, Mann-Whitney U test (median values for TGT), or log-rank test (actuarial estimates for time to local tumor recurrence were obtained using the Kaplan-Meier method; GraphPad Prism software version 4.03).

Acknowledgments

We thank Eric J. Bernhard, Erik H.J. Danen, and Kyle Legate for critical discussions and reading of the manuscript. We further thank Inga Lange and Daniela Tschuck for technical assistance and James Raleigh for the pimonidazole antibody. This work was supported in part by the Bundesministerium für Bildung und Forschung (to M. Baumann and N. Cordes), Deutsche Forschungsgemeinschaft grant Ba1433/5 (to M. Baumann and D. Zips), Austrian Science Foundation grant SFB021 and the Max Planck Society (to R. Fassler), and Cancer Research UK Core funding to Lincolns Inn Fields Laboratories (to B. Larijani).

Received for publication September 4, 2009, and accepted in revised form April 28, 2010.

Address correspondence to: Nils Cordes, OncoRay — Center for Radiation Research in Oncology, Medical Faculty Carl Gustav Carus, Dresden University of Technology, Fetscherstrasse 74/PF 41, 01307 Dresden, Germany. Phone: 351.458.7401; Fax: 351.458.7311; E-mail: Nils.Cordes@Oncoray.de.

1. Hehlgans S, Haase M, Cordes N. Signalling via integrins: implications for cell survival and anticancer strategies. *Biochim Biophys Acta*. 2007; 1775(1):163–180.
2. Karnoub AE, Weinberg RA. Ras oncogenes: split personalities. *Nat Rev Mol Cell Biol*. 2008;9(7):517–531.
3. Nelson CM, Bissell MJ. Of extracellular matrix, scaffolds, and signaling: tissue architecture regulates development, homeostasis, and cancer. *Annu Rev Cell Dev Biol*. 2006;22:287–309.
4. Cordes N, Seidler J, Durzok R, Geinitz H, Brakebusch C. beta1-integrin-mediated signaling essentially contributes to cell survival after radiation-induced genotoxic injury. *Oncogene*. 2006; 25(9):1378–1390.
5. Jacks T, Weinberg RA. Taking the study of cancer cell survival to a new dimension. *Cell*. 2002; 111(7):923–925.
6. Bissell MJ. Modelling molecular mechanisms of breast cancer and invasion: lessons from the normal gland. *Biochem Soc Trans*. 2007;35(pt 1):18–22.
7. Baumann M, Krause M, Hill R. Exploring the role of cancer stem cells in radioresistance. *Nat Rev Cancer*. 2008;8(7):545–554.
8. Krause M, Zips D, Thames HD, Kummermehr J, Baumann M. Preclinical evaluation of molecular-targeted anticancer agents for radiotherapy. *Radiother Oncol*. 2006;80(2):112–122.
9. Sawyers C. Targeted cancer therapy. *Nature*. 2004; 432(7015):294–297.
10. Cordes N, Meineke V. Cell adhesion-mediated radioresistance (CAM-RR). Extracellular matrix-dependent improvement of cell survival in human tumor and normal cells in vitro. *Strahlenther Onkol*. 2003;179(5):337–344.
11. Janes SM, Watt FM. New roles for integrins in squamous-cell carcinoma. *Nat Rev Cancer*. 2006;6(3):175–183.
12. Hynes RO. Integrins: bidirectional, allosteric signaling machines. *Cell*. 2002;110(6):673–687.
13. Legate KR, Montanez E, Kudlacek O, Fassler R. ILK, PINCH and parvin: the tIPP of integrin signalling. *Nat Rev Mol Cell Biol*. 2006;7(1):20–31.
14. Zhang Y, Chen K, Guo L, Wu C. Characterization of PINCH-2, a new focal adhesion protein that regulates the PINCH-1-ILK interaction, cell spreading, and migration. *J Biol Chem*. 2002;277(41):38328–38338.
15. Chiswell BP, Zhang R, Murphy JW, Boggon TJ, Calderwood DA. The structural basis of integrin-linked kinase-PINCH interactions. *Proc Natl Acad Sci U S A*. 2008;105(52):20677–20682.
16. Tu Y, Li F, Wu C. Nck-2, a novel Src homology2/3-containing adaptor protein that interacts with the LIM-only protein PINCH and components of growth factor receptor kinase-signaling pathways. *Mol Biol Cell*. 1998;9(12):3367–3382.
17. Dougherty GW, Jose C, Gimona M, Cutler ML. The Rsu-1-PINCH1-ILK complex is regulated by Ras activation in tumor cells. *Eur J Cell Biol*. 2008; 87(8–9):721–734.
18. Bock-Marquette I, Saxena A, White MD, Dimaio JM, Srivastava D. Thymosin beta4 activates integrin-linked kinase and promotes cardiac cell migration, survival and cardiac repair. *Nature*. 2004;432(7016):466–472.
19. Delcommenne M, Tan C, Gray V, Rue L, Woodgett J, Dedhar S. Phosphoinositide-3-OH kinase-dependent regulation of glycogen synthase kinase 3 and protein kinase B/AKT by the integrin-linked kinase. *Proc Natl Acad Sci U S A*. 1998;95(19):11211–11216.
20. Amaravadi R, Thompson CB. The survival kinases Akt and Pim as potential pharmacological targets. *J Clin Invest*. 2005;115(10):2618–2624.
21. Manning BD, Cantley LC. AKT/PKB signaling: navigating downstream. *Cell*. 2007;129(7):1261–1274.
22. Kim IA, et al. Selective inhibition of Ras, phosphoinositide 3 kinase, and Akt isoforms increases the radiosensitivity of human carcinoma cell lines. *Cancer Res*. 2005;65(17):7902–7910.
23. Milburn CC, Deak M, Kelly SM, Price NC, Alessi DR, Van Aalten DM. Binding of phosphatidylinositol 3,4,5-trisphosphate to the pleckstrin homology domain of protein kinase B induces a conformational change. *Biochem J*. 2003;375(pt 3):531–538.
24. Boudeau J, Miranda-Saavedra D, Barton GJ, Alessi DR. Emerging roles of pseudokinases. *Trends Cell Biol*. 2006;16(9):443–452.
25. Alessi DR, et al. Characterization of a 3-phosphoinositide-dependent protein kinase which phosphorylates and activates protein kinase Balpha. *Curr Biol*. 1997;7(4):261–269.
26. Jacinto E, et al. SIN1/MIP1 maintains rictor-mTOR complex integrity and regulates Akt phosphorylation and substrate specificity. *Cell*. 2006;127(1):125–137.
27. Yin Y, Shen WH. PTEN: a new guardian of the genome. *Oncogene*. 2008;27(41):5443–5453.
28. Xu W, et al. The heat shock protein 90 inhibitor geldanamycin and the ErbB inhibitor ZD1839 promote rapid PP1 phosphatase-dependent inactivation of AKT in ErbB2 overexpressing breast cancer cells. *Cancer Res*. 2003;63(22):7777–7784.
29. Cohen PT. Protein phosphatase 1--targeted in many directions. *J Cell Sci*. 2002;115(pt 2):241–256.
30. Gonzalez AM, Claiborne J, Jones JC. Integrin cross-talk in endothelial cells is regulated by protein kinase A and protein phosphatase 1. *J Biol Chem*. 2008;283(46):31849–31860.
31. Guo CY, Brautigan DL, Larner JM. Ionizing radiation activates nuclear protein phosphatase-1 by ATM-dependent dephosphorylation. *J Biol Chem*. 2002;277(44):41756–41761.
32. Wakula P, Beullens M, Ceulemans H, Stalmans W, Bollen M. Degeneracy and function of the ubiquitous RVXF motif that mediates binding to protein phosphatase-1. *J Biol Chem*. 2003; 278(21):18817–18823.
33. Dewhirst MW, Cao Y, Moeller B. Cycling hypoxia and free radicals regulate angiogenesis and radiotherapy response. *Nat Rev Cancer*. 2008;8(6):425–437.
34. Calleja V, Laguerre M, Parker PJ, Larijani B. Role of a novel PH-kinase domain interface in PKB/Akt regulation: structural mechanism for allosteric inhibition. *PLoS Biol*. 2009;7(1):e17.
35. Calleja V, et al. Intramolecular and intermolecular interactions of protein kinase B define its activation in vivo. *PLoS Biol*. 2007;5(4):e95.
36. Fernandez JJ, Candenas ML, Souto ML, Trujillo MM, Norte M. Okadaic acid, useful tool for studying cellular processes. *Curr Med Chem*. 2002;9(2):229–262.
37. Mitsuhashi S, Matsuura N, Ubukata M, Oikawa H, Shima H, Kikuchi K. Tautomycetin is a novel and specific inhibitor of serine/threonine protein phosphatase type 1, PP1. *Biochem Biophys Res Commun*. 2001;287(2):328–331.
38. Lange A, Wickström SA, Jakobson M, Zent R, Sainio K, Fässler R. Integrin-linked kinase (ILK) is an adaptor with essential functions during mouse development. *Nature*. 2009;461(7266):1002–1006.
39. Fukuda T, Chen K, Shi X, Wu C. PINCH-1 is an obligate partner of integrin-linked kinase (ILK) functioning in cell shape modulation, motility, and survival. *J Biol Chem*. 2003;278(51):51324–51333.
40. Zips D, et al. Enhanced susceptibility of irradiated tumor vessels to vascular endothelial growth factor receptor tyrosine kinase inhibition. *Cancer Res*. 2005;65(12):5374–5379.
41. Yaromina A, et al. Pre-treatment number of clonogenic cells and their radiosensitivity are major determinants of local tumour control after fractionated irradiation. *Radiother Oncol*. 2007;83(3):304–310.
42. Weaver VM, Fischer AH, Peterson OW, Bissell MJ. The importance of the microenvironment in breast cancer progression: recapitulation of mammary tumorigenesis using a unique human mammary epithelial cell model and a three-dimensional culture assay. *Biochem Cell Biol*. 1996;74(6):833–851.
43. Park CC, Zhang HJ, Yao ES, Park CJ, Bissell MJ. Beta1 integrin inhibition dramatically enhances radiotherapy efficacy in human breast cancer xenografts. *Cancer Res*. 2008;68(11):4398–4405.
44. Eke I, Sandfort V, Mischkus A, Baumann M, Cordes N. Antiproliferative effects of EGFR tyrosine kinase inhibition and radiation-induced genotoxic injury are attenuated by adhesion to fibronectin. *Radiother Oncol*. 2006;80(2):178–184.
45. Kadrmas JL, Beckerle MC. The LIM domain: from the cytoskeleton to the nucleus. *Nat Rev Mol Cell Biol*. 2004;5(11):920–931.
46. Vaynberg J, et al. Structure of an ultraweak protein-protein complex and its crucial role in regulation of cell morphology and motility. *Mol Cell*. 2005;17(4):513–523.

47. Stanchi F, et al. Consequences of loss of PINCH2 expression in mice. *J Cell Sci*. 2005;118(pt 24): 5899–5910.
48. Li F, Zhang Y, Wu C. Integrin-linked kinase is localized to cell-matrix focal adhesions but not cell-cell adhesion sites and the focal adhesion localization of integrin-linked kinase is regulated by the PINCH-binding ANK repeats. *J Cell Sci.* 1999;112(pt 24):4589–4599.
49. Hannigan GE, et al. Regulation of cell adhesion and anchorage-dependent growth by a new beta 1-integrin-linked protein kinase. *Nature*. 1996; 379(6560):91–96.
50. Hennessy BT, Smith DL, Ram PT, Lu Y, Mills GB. Exploiting the PI3K/AKT pathway for cancer drug discovery. *Nat Rev Drug Discov*. 2005;4(12):988–1004.
51. Hehlgans S, Eke I, Deuse Y, Cordes N. Integrin-linked kinase: dispensable for radiation survival of three-dimensionally cultured fibroblasts. *Radiother Oncol*. 2008;86(3):329–335.
52. Eke I, Leonhardt F, Storch K, Hehlgans S, Cordes N. The small molecule inhibitor QLT0267 Radiosensitizes squamous cell carcinoma cells of the head and neck. *PLoS One*. 2009;4(7):e6434.
53. Shevchenko A, et al. Chromatin Central: towards the comparative proteome by accurate mapping of the yeast proteomic environment. *Genome Biol.* 2008;9(11):R167.
54. King TD, Gandy JC, Bijur GN. The protein phosphatase-1/inhibitor-2 complex differentially regulates GSK3 dephosphorylation and increases sarcoplasmic/endoplasmic reticulum calcium ATPase 2 levels. *Exp Cell Res*. 2006;312(18):3693–3700.
55. Haase M, Gmach CC, Eke I, Hehlgans S, Baretton GB, Cordes N. Expression of integrin-linked kinase is increased in differentiated cells. *J Histochem Cytochem*. 2008;56(9):819–829.